3D displays: toward holographic video displays of 3D images

Pochi Yeh[1] **and Claire Gu**[2*]

[1]*Electrical and Computer Engineering, University of California Santa Barbara, California 93106, USA*

[2]*Electrical Engineering University of California Santa Cruz, California 95064, USA*

[*]*Corresponding author: claire@soe.ucsc.edu*

As the flat panel displays (Liquid Crystal Displays, AMOLED, etc.) reach near perfection in their viewing qualities and display areas, it is natural to seek the next level of displays, including 3D displays. There is a strong surge in 3D liquid crystal displays as a result of the successful movie *Avatar*. Most of these 3D displays involve the employment of special glasses that allow one view perspective for each of the eyes to achieve a depth perception. Such displays are not real 3D displays. In fact, these displays can only provide one viewing perspective for all viewers, regardless of the viewer's position. In addition, a fundamental viewing problem of focusing and accommodation exist that can lead to discomfort and fatigue for many viewers. In this paper, the authors review the current status of stereoscopic 3D displays and their problems. The authors will also discuss the possibility of using flat panels for the display of both phase and intensity of video image information, leading to the ultimate display of 3D holographic video images. Many of the fundamental issues and limitations will be presented and discussed.

1. Introduction

Display of information or images is an important part of our daily lives. As a result of their light weight, high quality and low power consumption, flat panel displays, especially liquid crystal displays (LCDs) are becoming the dominant display systems for mobile devices, home televisions and computer monitors. The success is a result of many contributing factors. These include the development of liquid crystal (LC) materials that offer a large electro-optical effect at low driving voltages, the development of active-matrix addressing using arrays of semiconductor thin film transistors (TFTs), the development of large area thin film polymers with superior birefringent optical properties, a good understanding of the transmission of polarized light in LCDs, and a growing demand for high-quality flat-panel displays in a broad area of applications, etc[1−3]. In the early days of liquid crystal displays, the viewing quality (in terms of contrast ratio and color stability) degrades at large viewing angles. This is mainly due to the leakage of light at the dark state of the display. The technology of polarization interference filters using birefringent crystals developed earlier for astrophysics plays a key role in the design of optical compensators for the improvement of viewing quality in LCDs[2,3]. In recent years, the defect problems in active-matrix organic light emitting displays (AMOLED) are mostly resolved. By virtue of its light emission nature, there is no leakage problem in AMOLED. As a result, AMOLEDs are capable of displaying high quality images with superior color stability and contrast ratios. Furthermore, the fast response of the emission process in AMOLEDs eliminates the problem of motion blur that occurs in LCDs. Flat panel displays, dominated by liquid crystal displays, are reaching near perfection in both the viewing qualities and display areas. The next generation flat panel displays should be able to display real 3D video images.

2. Current 3D displays and issues

3D movies that require special glasses have been around for over a hundred years. The recent success in liquid crystal displays, retardation films and polarizers makes it possible for the development of flat panel stereoscopic 3D video images. In addition, high speed scanning of laser beams can be employed for the volumetric display of 3D images[4]. Image pixels of a 3D object are projected via a scanning laser beam on a diffuser screen which is spun at high speed. The volumetric display of 3D images, however, requires a cubic volume of space needed to accommodate the spinning of the diffuser screen.

The stereoscopic display of 3D images can be achieved via a flat panel (e.g., LCD panel) in conjunction with a pair of special glasses that consist of synchronized shutters, orthogonal polarizers or color filters. Special glasses are not needed in auto-stereoscopic 3D display panels. However, the image quality is severely degraded in such displays. Fundamental problems exist in the viewing of stereoscopic 3D display of images. In stereoscopic 3D displays, two images are displayed either in sequence or simultaneously in different polarization states, one for each of the eyes. The viewers must focus (accommodate) their eyes on the screen where the light of the two images comes from. At the same time, the eyes must converge to the apparent location of the 3D image which can be either in front of the screen of behind the screen. Such a simultaneous effort of trying to converge and to accommodate with a different distance is a major source of eye discomfort and fatigue[5,6].

From the fundamental point of view, the stereoscopic display of 3D images provides only a depth perception.

It's not a display of real 3D images. The one single viewing perspective of stereoscopic display is defined by the two camera lenses that are employed to record the images. So, there's only one single viewing perspective in stereoscopic display. All viewers at different viewing positions see exactly the same 3D images. This may not be a problem for stationary viewers (e.g., in a movie theater). However, for home TVs, the single viewing perspective creates a problem for a viewer who may be moving around (e.g., in a living room). As we move, objects that are closer to us move farther across our field of view than do objects that are in the distance. This is known as motion parallax. So, for a moving viewer, the single viewing perspective in stereoscopic display creates an immediate conflict with the depth cue due to motion parallax. The conflict of viewing information in human brain can also cause discomfort, fatigue, or motion sickness.

In view of the fundamental problems in stereoscopic display, it is important to consider the possibility of flat panel display of real 3D images. From the optical point of view, the only real 3D images that can be displayed by a flat panel are holographic in nature. In the original invention of holograms, Gabor proposed the recording of 3D images in a planar recording medium via the employment of a reference beam in addition to the object beam[7]. As a result of optical interference, both amplitude and phase information of the object beam are recorded. In conventional imaging (photography), only the amplitude information of the object is recorded. As a result of the "total" recording of the object information in holography, the entire field (amplitude and phase) of the object beam is stored in the recording medium which can be a thin film or an array of photo-detectors. The reconstruction of the 3D object field is achieved by illuminating the recording medium with a reference beam. The reconstructed optical image is a real 3D image which can be viewed at various viewing perspectives. Although a number of special cases have been considered[8−10], a general investigation is not available. To illustrate this situation, we may point out, as an example, that the present state of the development does not address the issue of fundamental optical distortion due to magnification or demagnification via imaging lenses. In what follows, the authors will describe the possibility of combining holography and flat panels (e.g., liquid crystal displays (LCDs) or micro-electromechanical systems (MEMS)) for the display of real 3D images.

3. Holographic 3D displays

From the optical point of view, the field of light carrying the image of a 3D object can be written $E(x, y, z) = A(x, y, z) \exp[-ikz - i\phi(x, y, z)]$, where $A(x, y, z)$ is known as the amplitude and $\phi(x, y, z)$ is known as the phase. The propagation of this electric field in space is governed by Maxwell's equations (or wave equation). Using phasor notation, the field is often written as $E(x, y, z) = \psi(x, y, z) \exp[-ikz]$, where $\psi(x, y, z)$ is the complex amplitude that includes both the real amplitude and the phase. Here we assume that the object field is propagating in the positive z direction with k as the wave number. We no-

tice that the object field (or image field) is a three-dimensional function. In conventional imaging (photography), the film or photo-detector array records the intensity of the field (beam) at the image plane (say, $z=0$). The intensity recorded can be written $I(x, y, z = 0) = K|A(x, y, z = 0)|^2 = K|\psi(x, y, z = 0)|^2$, where K is a constant. This is a 2D image. The conventional recording completely ignores the phase information at the image plane $\phi(x, y, z = 0)$. Without the phase information, it is impossible to reconstruct (display) the 3D images.

Using Gabor's holographic recording scheme with the help of a reference beam, it is possible to record the field (both amplitude and phase) of the image at the image plane ($z=0$). This field is often written as $E_0(x, y) = A_0(x, y) \exp[-i\phi_0(x, y)]$, where $E_0(x, y) = E(x, y, z = 0)$, $A_0(x, y) = A(x, y, z = 0)$ and $\phi_0(x, y) = \phi(x, y, z = 0)$. It is important to note that the "image" plane ($z=0$) in holographic recording can be arbitrary. The choice of location of the plane for holographic recording of the object field depends on applications. This field can be reconstructed via the illumination of a beam of light. Upon reconstruction, the field $E_0(x, y) = A_0(x, y) \exp[-i\phi_0(x, y)]$ is generated at $z=0$. Although this is a two-dimensional function, the entire original field $E(x, y, z) = A(x, y, z) \exp[-ikz - i\phi(x, y, z)]$ can be obtained as the field propagates in space. As a result, a real 3D image of the original object is obtained. This is the basic principle of holographic recording and reconstruction. In this section, the authors will describe the possibility of using such recording scheme and using flat panels that are capable of displaying both amplitude and phase information for the holographic video display of 3D images. Among the most popular flat panel displays, liquid crystal displays (LCDs) and micro-electromechanical systems (MEMSs) are capable of displaying both the amplitude and phase. Although AMOLEDs can offer excellent picture quality, they are unable to display phase information.

There are several fundamental steps that are needed for the ultimate holographic 3D display of video images. These include the following: a) the holographic recording of the object field, b) the conversion of the recorded field into video signals of amplitude and phase, c) the input of the video signals into a holographic display unit. Referring to Figure 1, we consider a schematic drawing of a holographic recording of the object field.

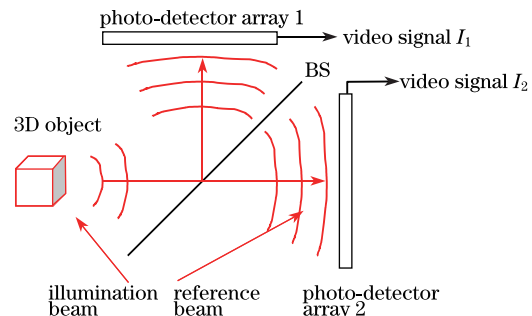In the holographic recording, the object must be

Fig. 1. Schematic drawing of a holographic recording system. The recorded intensity patterns are converted into digital signals in the electronic domain.

illuminated by a spatially coherent beam of light. The optical field of the object consists of light reflected and/or scattered from the object and collected by the recording element (e.g., a photo-detector array). Optional lens system can be employed for the purpose of energy efficiency. Before reaching the recording element, the optical wave of the object field is split into two by a beam splitter. Each of these two parts is then directed toward a photodetector array. As shown in Figure 1, a reference beam (usually a plane wave) is employed for the holographic recording in one of the photo-detector arrays (e.g., array 2 in Figure 1). In such a recording scheme, the recorded intensities at the detector arrays can be written, respectively

$$I_1(x,y) = K|E_0(x,y)|^2 = KA_0^2(x,y),$$

$$I_2(x,y) = K|E_0(x,y) + \mathrm{Re}^{-\mathrm{i}\alpha x - \mathrm{i}\beta y}|^2$$
$$= K\{A_0^2(x,y) + R^2 + 2RA_0(x,y)$$
$$\cdot \cos[\phi_0(x,y) - \alpha x - \beta y]\}, \quad (1)$$

where $\mathrm{Re}^{-\mathrm{i}\alpha x - \mathrm{i}\beta y}$ is the field of the reference beam at the recording plane (z=0) with α and β as constant representing the x- and y-components of the wave vector, respectively, and R as the amplitude of the reference beam. We may assume β=0 without loss of generality. The measured intensity distributions are electronically (digitally) recorded and stored.

From these two sets of the digitally stored intensity patterns, we obtain

$$A_0(x,y) = \sqrt{I_1(x,y)/K},$$

$$\phi_0(x,y) = \cos^{-1}\left(\frac{I_2(x,y) - I_1(x,y) - KR^2}{2R\sqrt{KI_1(x,y)}}\right) + \alpha x + \beta y,$$
$$(2)$$

In other words, both the amplitude and the phase of the object field at the plane (z=0) of the detector array are obtained by using the recording scheme shown in Fig. 1. These two sets of digital data are in the electronic domain. They represent the video signal of the 3D image of the object. Although a single photodetector array is sufficient in the conventional holographic recording, the holographic recording scheme invloving two photodetector arrays described in Figure 1 provides the benefit of less computation time for obtaining both the phase and amplitude information of the object field.

If the video signal of the amplitude and the phase as described in Eq. (2) can be fed to a flat panel display unit such as a liquid crystal (LC) panel, then a holographic 3D image of the object field can be displayed via the illumination of a spatially coherent reference beam, provided the display unit is capable of faithfully displaying both the amplitude and the phase information. Such a 3D image is a real 3D image with all the viewing perspectives and depth of field (focus). Generally speaking, there are two ways of reconstructing (displaying) the object field as illustrated below. Figure 2 shows a reconstruction scheme employing a read beam which is identical to the reference beam. If the video signal I_2 obtained in Fig. 1 is directly fed to the holographic display unit,
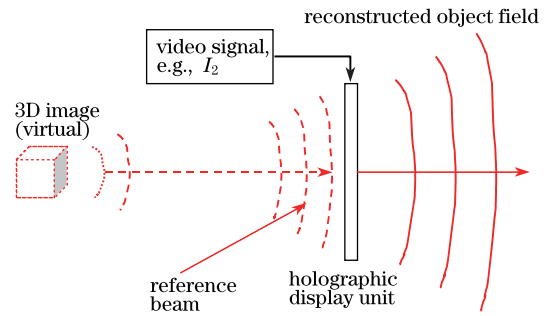

Fig. 2. Schematic drawing of a reconstruction of the object field that produces a 3D virtual image having all the viewing perspectives and depth of field (focus). The video signal I_2 obtained in Fig. 1 is now fed to the holographic display unit as a video input signal.

phase compensators may be required to compensate for the phase variation which is a side product of intensity variation of a liquid crystal display (e.g., in TN-LCDs and VA-LCDs).

Upon illumination by the read beam, the object field at the plane of display unit (z=0) is reconstructed. This is the field $E_0(x,y) = A_0(x,y)\exp[-\mathrm{i}\phi_0(x,y)]$ at z=0. This field will propagate in the positive z-direction. Let the field for an arbitrary z be written $E(x,y,z) = \psi(x,y,z)\exp[-\mathrm{i}kz]$, where $\psi(x,y,z)$ is the complex amplitude (including the phase) of the field. The propagation in space is governed by[8,9]

$$\frac{\partial}{\partial z}\psi(x,y,z) = \frac{1}{2\mathrm{i}k}\left(\frac{\partial^2}{\partial x^2} + \frac{\partial^2}{\partial y^2}\right)\psi(x,y,z). \quad (3)$$

Eq. (3) governs the propagation of the object field in one direction once the field at $z = 0$ is given. It's an approximation known as the "slowly varying amplitude approximation," or simply the parabolic approximation[11,12]. The second order transverse derivatives on the right-hand side account for the diffraction of the beam. The first order derivative on the left side accounts for the change of the field amplitude due to the diffraction. Such a reconstruction produces the object field that propagates to the right of the holographic display unit. The reconstructed object field appears to be originated from the original object location. The virtual 3D image exhibits all the viewing perspectives simultaneously and depth of field (focus). Optical imaging lens system can be employed for re-imaging purpose so that the final 3D image appears at a desired location.

The propagation of the object field from the display unit at $z = 0$ to any location z can also be described by using the Fresnel–Kirchhoff integral[13],

$$\psi(x,y,z) = \frac{\mathrm{i}}{\lambda z}\mathrm{e}^{-\mathrm{i}kz}\iint\psi(x',y')\mathrm{e}^{-\mathrm{i}k\frac{(x-x')^2+(y-y')^2}{2z}}\,\mathrm{d}x'\mathrm{d}y'.$$
$$(4)$$

The integral can be evaluated using computers. In the field of digital holography[14,15], the reconstruction of the object field, which is done optically by illumination of a hologram, is performed by numerical methods. The reconstruction process is based on the numerical integration of the Fresnel–Kirchhoff integral shown above. Digital holography also offers the possibility of computer generated holograms (CGH) which can be useful for the
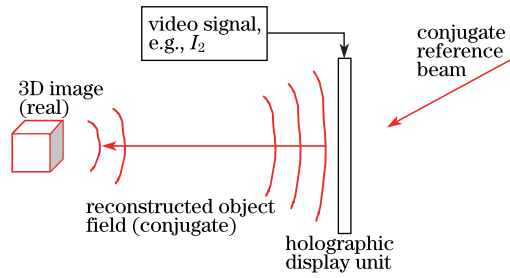
Fig. 3. Schematic drawing of a reconstruction of the conjugate object field that produces a 3D real image having all the viewing perspectives and depth of field (focus).

creation of 3D images for video games. However, for the purpose of the display of a real 3D image of the object, such a computation is not needed. The propagation in space as governed by Eqs. (3, 4) will automatically generate the real 3D image needed for the display, provided the display unit is capable of faithfully displaying both the amplitude and the phase information.

Figure 3 shows a reconstruction scheme employing a read beam which is a phase conjugate of the reference beam. Upon illumination by the conjugate reference beam, the conjugate object field at the plane of display unit (z=0) is reconstructed. This is the field $E_0^*(x,y) = A_0^*(x,y) \exp[+\mathrm{i}\phi_0(x,y)]$ at z=0. This field will propagate in the negative z-direction, retracing the original object wave and producing a real 3D image of the conjugate object at the original location of the object. The real 3D image exhibits all the viewing perspectives simultaneously and depth of field (focus). Again, optical imaging lens system can be employed for re-imaging purpose so that the final 3D image appears at a desired location.

In the above discussion of 3D holographic recording and display, we made several assumptions. These include the availability of spatially coherent beams for illumination as well as for reference, the availability of photo-detector arrays and display unit with pixel sizes smaller than the characteristic length of variation of the phase and amplitude information as given by Eq. (2). In what follows, the authors will address some of the fundamental issues and limitations involved in 3D holographic display of video images.

4. Technical issues

One of the most difficult technical issues will be the availability of display unit with pixel sizes that are in the sub-micron ranges. It is important to note that there are no fundamental limitation of making sub-micron pixel electrodes. Current photolithography is capable of making electrodes as small as 50 nm or less. Each liquid crystal cell (pixel) in a liquid crystal panel is capable of displaying both the phase and the amplitude of a transmitted (or reflected) beam. In conventional liquid crystal displays (e.g., vertically aligned (VA)), the typical pixels are about 100 μm with a cell gap of about 3~5 μm. In such a geometry, the physical region of the fringing field is relatively small. However, if the pixel size is sub-micron while the cell gap is of the order of one micron, then the field between the conductors is mostly fringing field. This is a direct consequence of $\nabla \times \mathbf{E} = 0$.

In the following analysis, we assume that such display units with sub-micron pixels are available. As a result of the sub-micron pixels, there are several technical issues that are affecting the performance of the display unit. These include the total number of pixels and the fringing field effect in liquid crystal display units. As a result of the high resolution (small pixels), the total number of pixels can exceed 100 million. Parallel driving of the whole panel via several TFT arrays is required. Also as the pixel becomes very small (smaller than the cell gap of liquid crystal panels) the presence of fringing field can not be ignored. As a result, the depth of phase modulation of a liquid crystal panel is limited to a small fraction of 2π. The liquid crystal hologram is thus considered a "thin" hologram. To illustrate this, we consider a thin liquid crystal layer sandwiched between transparent electrodes (see Fig. 4).

Referring to Fig. 4, we consider the electric field inside a pair of conductors. The upper conductor is continuous, while the lower conductor consists of an array of pixel conductors. The voltage applied to the lower conductor array can be written $V_0 \cos Kx$, while the upper conductor (the common conductor) is kept at zero voltage. Here we assume that the pixel dimension is small enough so that a continuous voltage function $V_0 \cos Kx$ is a good representation. For the purpose of illustration, we assume a periodic voltage function with a period of $\Lambda = 2\pi/K$ with $\Lambda << d$, where d is the cell gap. In this approximation, the solution of the field inside the conductors can be written as

$$\begin{cases} E_x = KV_0\mathrm{e}^{-Kz}\sin Kx \\ E_z = KV_0\mathrm{e}^{-Kz}\cos Kx \end{cases}, \tag{5}$$

We notice that the field decays exponentially as a function of z. In the region near the top conductor, the electric field is near zero. For such a structure, the effective thickness of electro-optical modulation is limited to a thickness of $d_{\mathrm{eff}} = 1/K$. As a result the effective phase modulation depth is limited to $k\Delta n d_{\mathrm{eff}} = k(n_{\mathrm{e}}-n_{\mathrm{o}})/K = (n_{\mathrm{e}}-n_{\mathrm{o}})\Lambda/\lambda$. In other words, the phase modulation depth is capped at $(n_{\mathrm{e}}-n_{\mathrm{o}}) = \Lambda/\lambda$ for any cell gap greater than $d_{\mathrm{eff}} = 1/K$. For most liquid crystal materials, $(n_{\mathrm{e}} - n_{\mathrm{o}})$ is around 0.1. So, for high resolution holograms with Λ in the submicron range, the phase modulation depth is a small fraction of 2π. For the purpose of holographically reconstructing the 3D image of the object field, a phase modulation depth of 2π is not needed. However, the small depth of modulation leads to a small diffraction efficiency (small energy efficiency) when the 3D images are reconstructed.

In what follows, we consider the reconstruction of the object field via the diffraction of the read beam by a liquid crystal panel that display both the amplitude and
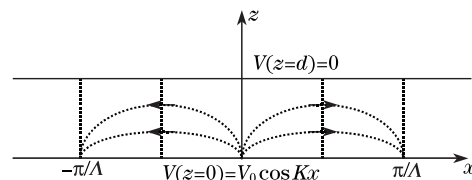

Fig. 4. Electric field lines inside a liquid crystal cell where the cell gap is much larger than the pixel dimension.
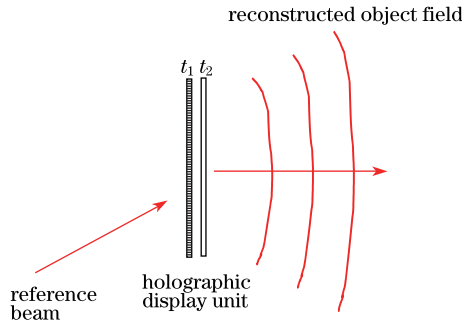
Fig. 5. Schematic drawing of the reconstruction of the field of 3D object via the employment of a readout beam and a display unit consisting of an amplitude-only display panel and a phase-only display panel.

the phase of the object field recorded at location $z = 0$. Referring to Fig. 5, we consider the case where the liquid crystal panel consists of two sub-panels in sequence for the purpose of illustrating the concept. In practice, an integrated flat panel is sufficient provided that the panel is capable of displaying independently the phase and amplitude information.

The first panel is an amplitude panel with a transmission coefficient of

$$t_1(x, y) = CA_0(x, y), \tag{6}$$

where C is a constant and $A_0(x, y)$ is the recorded amplitude according to Eq. (2). The second panel is a phase panel with a transmission coefficient of

$$t_2(x, y) = \mathrm{e}^{-\mathrm{i}\delta_0 - \mathrm{i}\delta_1 \cos[\phi_0(x,y) - \alpha x - \beta y]}, \tag{7}$$

where δ_0, δ_1 are constants, $\phi(x, y)$ is the recorded phase information of the object field according to Eq. (2). Physically, the second panel (phase panel) is a hologram containing the phase information of the object field. It consists of a phase grating (defined by the wave numbers α and β) modulated by the phase information $\phi(x, y)$ of the object field. Using the identity

$$\mathrm{e}^{-\mathrm{i}\delta \cos u} = \sum_{m=-\infty}^{\infty} J_m(\delta) \mathrm{e}^{\mathrm{i}mu} (-\mathrm{i})^m, \tag{8}$$

the transmission coefficient (shown in Eq. (7)) of the phase element can be written as

$$
\begin{aligned}
t_2(x, y) &= \mathrm{e}^{-\mathrm{i}\delta_0 - \mathrm{i}\delta_1 \cos[\phi_0(x,y) - \alpha x - \beta y]} \\
&= \mathrm{e}^{-\mathrm{i}\delta_0} [J_0(\delta_1) - \mathrm{i}J_1(\delta_1) \mathrm{e}^{-\mathrm{i}[\phi_0(x,y) - \alpha x - \beta y]} \\
&\quad + \mathrm{i}J_{-1}(\delta_1) \mathrm{e}^{+\mathrm{i}[\phi_0(x,y) - \alpha x - \beta y]}] \\
&\quad + \mathrm{e}^{-\mathrm{i}\delta_0} [-J_2(\delta_1) \mathrm{e}^{-\mathrm{i}2[\phi_0(x,y) - \alpha x - \beta y]} \\
&\quad - J_{-2}(\delta_1) \mathrm{e}^{+\mathrm{i}2[\phi_0(x,y) - \alpha x - \beta y]}] \\
&\quad + \mathrm{e}^{-\mathrm{i}\delta_0} [-\mathrm{i}J_3(\delta_1) \mathrm{e}^{-\mathrm{i}3[\phi_0(x,y) - \alpha x - \beta y]} \\
&\quad + J_{-3}(\delta_1) \mathrm{e}^{+\mathrm{i}3[\phi_0(x,y) - \alpha x - \beta y]}] \cdots\cdots. \tag{9}
\end{aligned}
$$

For small modulation depth ($\delta \ll 1$), the high order terms are small. Using a read beam of $S_0 \mathrm{e}^{-\mathrm{i}kz - \mathrm{i}\alpha x - \mathrm{i}\beta y}$,

the field of the diffracted beam at the right side of the plane of the panel ($z=0+$) can be written as

$$E_\mathrm{d}(x, y) = t_1(x, y) t_2(x, y) S_0 \mathrm{e}^{-\mathrm{i}\alpha x - \mathrm{i}\beta y}. \tag{10}$$

By using Eqs. (6–9), we obtain

$$
\begin{aligned}
E_\mathrm{d}(x, y) &= CA_0(x, y) S_0 \mathrm{e}^{-\mathrm{i}\delta_0} \lfloor J_0(\delta) - \mathrm{i}J_1(\delta) \mathrm{e}^{-\mathrm{i}\phi_0(x,y)} \rfloor \\
&\quad + \text{High order terms in } (\mathrm{e}^{-\mathrm{i}\alpha x - \mathrm{i}\beta y}). \tag{11}
\end{aligned}
$$

This field will propagate in the region ($z > 0$) according to Eq. (3). Among all the diffraction orders, the first order term is identical to that of the object field,

$$E_1(x, y, z) = -\mathrm{i}CJ_1(\delta) S_0 \mathrm{e}^{-\mathrm{i}\delta_0} A_0(x, y) \mathrm{e}^{-\mathrm{i}kz - \mathrm{i}\phi_0(x,y)}. \tag{12}$$

There are other diffraction orders that will propagate in different directions. The number of diffraction orders depends on the grating (hologram) period as well as the depth of modulation. It is possible to minimize or eliminate the additional diffraction orders by using thick holograms (e.g., MEMS with deep phase modulation). However, this is difficult for liquid crystal cells. Spatial filters can be employed to block these high diffraction orders. The diffraction efficiency for the reconstruction of the object field is proportional to $|J_1(\delta)|^2$.

According to Eq. (12), the first order diffraction beam reproduces the object field $E_0(x, y) = A_0(x, y) \exp[-\mathrm{i}\phi_0(x, y)]$ at $z=0$. This field will propagate in space as governed by Eq. (3) and reproduce the entire object field. As a result the 3D image of the original object is obtained. This 3D image exhibits all the viewing perspectives simultaneously and depth of field (focus). Flat panels of liquid crystal cells with sub-micron pixels suffer from the problem of low diffraction efficiency (energy efficiency) as a result of the low phase modulation depth discussed above.

Flat panels of MEMS are capable of providing a full phase modulation of 2π[16]. This requires a physical displacement of $\lambda/2$ (half-wavelength) for each of the micro-mirrors. Using such panels, a quasi-holographic display unit which consists of an amplitude-only display panel as given by Eq. (6) and a phase-only MEMS display unit with a transmission given by

$$t_2'(x, y) = \mathrm{e}^{-\mathrm{i}\phi_0(x,y)}, \tag{13}$$

can obtain a reconstruction of the object field via a direct illumination of the panels in the perpendicular direction as shown in Fig. 6.
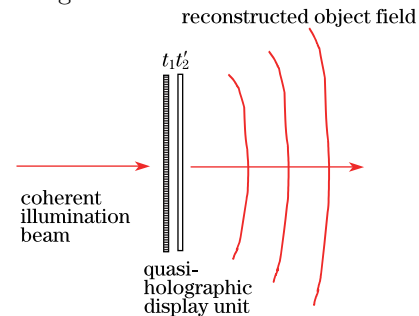

Fig. 6. Quasi-holographic display unit. The phase-only display unit in such a display scheme requires a full phase modulation depth of 2π for each of the pixels.

The phase element t'_2 in the quasi-holographic scheme described in Fig. 6 usually involves lower spatial frequency than that of the grating (α, β), depending on the complexity of the object. As a result, the stringent requirement for the small pixel sizes can be somewhat relaxed. This can be extremely important in the manufacturing of the panels as well as the reduction of the total number of pixels. In what follows, we consider a fundamental optical issue of distortion and other technical issues.

5. Fundamental optical issues

For practical purposes, it is essential to enlarge or shrink the 3D images. For example, we need to shrink the 3D images of a sport event (e.g., football games) so that the 3D images are small enough to appear inside a living room. This is relatively easy in 2D images by using optical lens systems. However, for 3D images, an intrinsic distortion occurs. It is known in conventional imaging optics that the longitudinal magnification is different from the transverse magnification. They are related by the following relationship[17]:

$$M_{\text{Longitudinal}} = M_{\text{Transverse}}^2. \tag{14}$$

For example, if we shrink the transverse dimension of the images by 10, then the same images are shrunk by a factor of 100 in the longitudinal dimension. Furthermore, the magnification may depend on the exact longitudinal location of the 3D object/image. In other words, each longitudinal part of the 3D object has a different magnification factor. This dependence and the disparity of the longitudinal/transverse magnification lead to a distortion of the 3D images. The 3D image can be stretched asymmetrically as a result of the imaging demagnification or magnification. In $4f$ imaging systems involving a pair of confocal lenses, the magnification is independent of the longitudinal position. However, the condition Eq. (14) still applies. As a result, the 3D images are compressed in the longitudinal direction after demagnification. Such an optical distortion is fundamental in optical lens systems. The only way to compensate such a distortion is to employ something other than optical lenses. This includes digital holographic computation involving a Fresnel-Kirchoff transformation and an inverse Fresnel-Kirchoff transformation to reformat the signal in the electronic domain. An example is described as follows.

Referring to Fig. 7, we consider a field amplitude $\psi_1(x_1, y_1)$ at $z = 0$ which upon propagation will generate a 3D image $f_1(x_1, y_1, z = z_1)$ at location $z = z_1$, and a field amplitude $\psi_2(x_2, y_2)$ at $z = 0$ which upon propagation will generate a 3D image $f_2(x_2, y_2, z = z_2)$ at location $z = z_2$. Further, we assume that the 3D image at $z = z_2$ is a scaled version (magnified or demagnified) of the 3D image at $z = z_1$. Mathematically, this is written $f_2(x_2, y_2, z = z_2) = f_1(sx_1, sy_1, z = z_1)$, where s is the scale factor.

We assume that the field amplitude $\psi_1(x_1, y_1)$ at $z = 0$ for object 1 is obtained via holographic recording. This field amplitude is capable of reproducing a 3D image of object 1 at $z = z_1$. The field amplitude of this 3D image
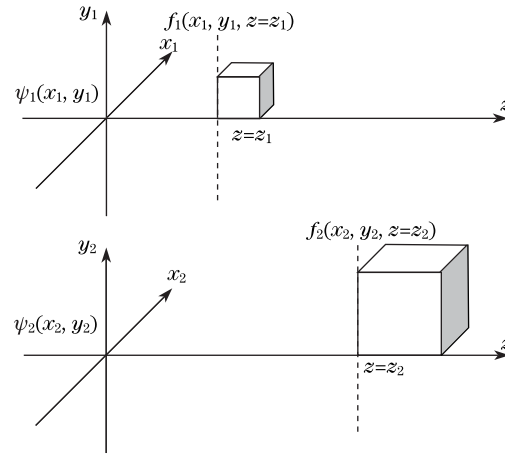

Fig. 7. Schematic drawing of Fresnel-Kirchoff propagation for the formation of 3D images.

$f_1(x_1, y_1, z = z_1)$ at $z = z_1$ can be obtained via the Fresnel-Kirchoff transformation integral of Eq. (4). Conversely, the field amplitude $\psi_1(x_1, y_1)$ at $z = 0$ can be obtained via an inverse Fresnel-Kirchoff transformation of $f_1(x_1, y_1, z = z_1)$. Similarly, the field amplitude $\psi_2(x_2, y_2)$ at $z = 0$ can be obtained via an inverse Fresnel-Kirchoff transformation of $f_2(x_2, y_2, z = z_2)$. If we set $f_2(x_2, y_2, z = z_2) = f_1(sx_1, sy_1, z = z_1)$, then we will obtain the field amplitude $\psi_2(x_2, y_2)$ at $z = 0$ that is capable of producing a scaled image at location $z = z_2$. This approach of scaling the image size may not be subject to the distortion as described in Eq. (14). However, a distortion is still possible. Further analysis to quantify the distortion is needed. This is only an example of reformating the signal in the electronic domain.

There are several other issues. These include the spatial coherent light source that is needed for the holographic recording as well as holographic readout. At the moment, there's no flat panel spatially coherent light source. Such a flat panel spatially coherent light source can be obtained via several methods. For example, a laser beam coupled into a single mode thin film waveguide with a tapered grating on one side of the film. By proper design of the tapering, it is possible to redirect the coherent light out of the thin film waveguide leading to a flat panel of spatially coherent light source. It is also possible to achieve a spatially coherent light source via a 2D array of coupled VCSELs. The coherence is obtained via phase coupling in the lateral directions.

6. Conclusion

In summary, we proposed and discussed the possibility of holographic recording and display of 3D images for the ultimate flat panel display of video images. We described some of the most important technical issues involved in the holographic recording and display of 3D images. These include the phase modulation depth limitation of liquid crystal panels, the sub-micron pixels needed, the spatially coherent light needed, the fundamental optical distortion in conventional imaging and re-imaging for the purpose of magnification and demagnification. We also proposed and described a digital approach employing Fresnel-Kirchoff transformation and inverse Fresnel-Kirchoff transformation for the scaling of

the 3D images. Many of the enabling technologies must be developed for the ultimate demonstration of the holographic display of 3D video images.

References

1. H. Kawamoto, Proc. IEEE **90,** 460 (2002).
2. P. Yeh, Opt. Rev. **16,** 192 (2009).
3. P. Yeh and C. Gu, *Optics of Liquid Crystal Displays* (Wiley, 2009).
4. A. Sullivan, Spectrum IEEE **42,** 30 (2005).
5. D. M. Hoffman, A. R. Girshick, K. Akeley, and M. S. Banks, J. Vision 8 (2008).
6. M. Lambooij, M. Fortuin, I. Heynderickx, and W. I. Jsselsteijn, J. Imaging Science **53,** 30201 (2009).
7. D. Gabor, Nature **161,** 777 (1948).
8. N. Leister, G. Fütterer, R. Häussler, S. Reichelt, H. Sahm, A. Schwerdtner, A. Schwerdtner, and H. Stolle, IMID DIGEST 1179 (2009).
9. P.-A. Blanche, Information Display **28,** 32 (2012).
10. P.-A. Blanche, A. Bablumian, R. Voorakaranam, C. Christenson, W. Lin, T. Gu, D. Flores, P. Wang, W. Y. Hsieh, and M. Kathaperumal, Nature **468,** 80 (2010).
11. A. Yariv and P. Yeh, *Optical Waves in Crystals* (Wiley, 1984), p. 24.
12. P. Yeh, *Introduction to Photorefractive Nonlinear Optics* (Wiley, 1993), p. 11.
13. A. Yariv and P. Yeh, *Photonics: Optical Electronics in Modern Communications (The Oxford Series in Electrical and Computer Engineering)* (Oxford University Press, 2006).
14. U. Schnars and W. P. O. Jüptner, Meas. Sci. Technol. **13,** R85 (2002).
15. U. Schnars and W. Jüptner, *Digital Holography* (Springer, 2005).
16. D. M. Bloom, Proc. SPIE **3013,** 165 (1997).
17. O. S. Heavens and R. W. Ditchburn, *Insight into Optics*, (Wiley, 1991), pp. 19-23.